

A 2.60pJ/Inst Subthreshold Sensor Processor for Optimal Energy Efficiency

Bo Zhai, Leyla Nazhandali, Javin Olson, Anna Reeves, Michael Minuth, Ryan Helfand,
Sanjay Pant, David Blaauw and Todd Austin

University of Michigan, Ann Arbor, MI

Abstract

A 2.6pJ/Inst subthreshold sensor processor designed for energy efficiency has been fabricated. A two-stage micro-architecture was implemented to mitigate the impact of process variation in subthreshold operation. Careful library cell selection and robust SRAM design enabled fully functional operation from 1.2V to 200mV. We analyze the variation in frequency and optimal voltage and evaluate the need for adaptive control. The processor reaches maximum energy efficiency at 360mV, consuming 2.6pJ/Inst at 833kHz. The minimum energy consumption of the core marks a 10X improvement over previous sensor processors at the same MIPS.

1. Introduction

Subthreshold circuit operation is a compelling method for ultra-low power sensor applications. In previous work [1], we demonstrated the existence of a so-called minimum energy voltage (V_{min}) where CMOS logic reaches maximum energy efficiency per operation. This occurs when leakage and dynamic energy are comparable. Scaling the supply voltage below V_{min} ceases to reduce energy per operation due to the dominance of leakage in this voltage regime, combined with the exponential increase of circuit delay with V_{dd} . Several previous subthreshold circuits [2][3] were presented. However, to our knowledge this paper presents the first silicon implementation and measurement of a general purpose sensor processor (referred to as the *Subliminal* processor) specifically optimized for energy efficient subthreshold operation.

2. Implementation for Optimal Energy Efficiency

For high energy efficiency in subthreshold operation, a CISC micro-architecture [4] as selected, which has an 8-bit wide ALU, a 32-bit accumulator and a unified instruction and data memory. The instruction set was optimized for both good code density and low complexity which helps achieve less energy consumption.

On-current variation increases significantly in subthreshold operation from $3\sigma/\mu=69\%$ at $V_{dd}=600\text{mV}$ to 225% at $V_{dd}=260\text{mV}$ for an individual $0.3\mu\text{m}$ wide NMOS transistor. However, in subthreshold operation the sensitivity to L_{eff} variation is reduced and the variation due to random dopant fluctuation (RDF) dominates [5]. Due to its uncorrelated nature, RDF average out over the length of a path making shallow pipelines with high FO4 delay per stage advantageous, as shown in Figure 1. Hence, a 2 stage pipeline implementation was selected for the processor, which shows a 14% reduction in $3\sigma/\mu$ of delay compared to a design with 10 FO4 delays.

For efficient subthreshold operation, all gates with more than 2 fan-ins were eliminated from the library as well as all pass-transistor logic and the library was re-characterized at subthreshold voltage. We found that a processor synthesized with this dedicated subthreshold library is $\sim 9\%$ faster at subthreshold voltage than one with a standard library, although both have the same performance at full V_{dd} . This is caused by the different scaling of cell delays with V_{dd} . Particularly, a 20% change in the beta ratio between 1.2V and 250mV caused an 18% change in the NAND / NOR cell delay ratio.

The 2kb SRAM was implemented using a custom designed, mux-based array structure. This resulted in a minimum functional voltage of 200mV, which is much lower than V_{min} . Hence, reducing the minimum functional voltage further is unnecessary.

A special level converter was implemented for the test harness to convert the 200mV signals to 1.2V using four differential sub-converter stages as shown in Figure 2. In order to suppress process variability and improve robustness, the first two sub-converter stages

were increased in size to reduce the impact of RDF and have body bias control to compensate for global beta-ratio shift.

Figure 3 shows the die photograph of the core and the memory. The test chip was fabricated in an industrial $0.13\mu\text{m}$ CMOS process with 8 layers of metal. The area of the processor core is $29817\mu\text{m}^2$ and the area of the SRAM is $55205\mu\text{m}^2$.

3. Measurement Results and Discussion

Figure 4 shows the maximum operating frequency with V_{dd} for 4 chips. As expected, the operating frequency drops rapidly below V_{th} ($\sim 400\text{mV}$). In Figure 5, we plot the energy per instruction with V_{dd} for one measured die. The minimum energy (E_{min}) occurs at $\sim 360\text{mV}$, where active energy (including short circuit current) and leakage have equal and opposite sensitivity to supply voltage, and leakage energy is $\sim 33\%$ of the total energy. Figure 6 shows the energy breakdown between the core and memory. V_{min} for the core falls at $\sim 280\text{mV}$ while that for the memory is much higher at $\sim 400\text{mV}$, due to its much lower activity rate.

In Figure 7, we show the measured operating frequency distribution of 26 chips at three voltages: 600mV, 400mV and 260mV. Table 1 shows the corresponding $3\sigma/\mu$ values which range from 29.6% to 85.5%. This marks a $\sim 2.63\text{X}$ improvement compared to the variation of individual devices, as shown in Section 2, and is due in part to the high logic depth in the *Subliminal* processor.

Figure 8 shows the V_{min} and E_{min} distributions of the *Subliminal* processor over 26 measured chips. The V_{min} ranges from 340mV to 420mV, with a mean and standard deviation of 378mV and 21.4mV, respectively ($3\sigma/\mu$ is 22.8%). The E_{min} per instruction ranges from 2.6pJ per instruction to 3.4pJ with a mean of 3.0pJ and standard deviation of 0.170pJ ($3\sigma/\mu$ is 16.99%). However, to obtain this minimum energy operation, each die must operate at its individual V_{min} and operation frequency which requires adaptive frequency and voltage tuning of each die. Hence, in Figure 8 we also show the energy distribution when all die operate at a fixed V_{dd} equal to $\mu(V_{min}) = 378\text{mV}$, resulting in a mean energy $\mu(E) = 3.19\text{pJ}$ (a 6% increase) and standard deviation $\sigma(E) = 0.21\text{pJ}$ (a 23% increase). This relatively small increase is the result of the low sensitivity of energy to voltage near V_{min} and the relatively small variation of V_{min} between different die. This leads to the useful observation that adaptive voltage tuning is only marginally beneficial for maximum energy efficiency in subthreshold operation. On the other hand, Figure 8 also shows the energy distribution when all die are operated at a fixed, worst-case ($\mu+3\sigma$) frequency in which case $\mu(E) = 3.72\text{pJ}$ (a 24% increase) and $\sigma(E) = 0.283\text{pJ}$ (a 66% increase). Hence, more significant energy savings are obtained by applying adaptive frequency tuning in subthreshold design.

The energy consumption of four sensor application programs is shown in Figure 9. The variation in their individual energy demands was reduced in subthreshold operation due to the increased contribution of application-independent leakage current. Furthermore, the applications showed nearly identical V_{min} .

Finally, we compare the energy-per-instruction and MIPS of the *subliminal* processor with those of *Hempstead* [6], *cleverDust* [7] and *SNAP/LE* [8] in Figure 10. The energy consumption of memory is not included in Figure 10 because previous efforts only reported data for the core. The *Subliminal* processor consumes 0.86pJ per instruction at 0.04 MIPS and 1.2pJ at 0.5 MIPS which marks a more than 10X reduction compared to the previous best *cleverDust* processor at equal MIPS.

References

- [1] B. Zhai, *et al.*, DAC, 2004
 [2] C.H.-I. Kim, *et al.*, TVLSI 2003
 [3] A. Wang, *et al.*, ISSCC 2004
 [4] L. Nazhandali, *et al.*, ISCA 2005
 [5] B. Zhai, *et al.* ISLPED 2005
 [6] M. Hempstead, *et al.*, ISCA 2005
 [7] B. A. Warneke *et al.*, ISSCC 2004
 [8] V. Ekanayake, *et al.*, ASPL, 2004

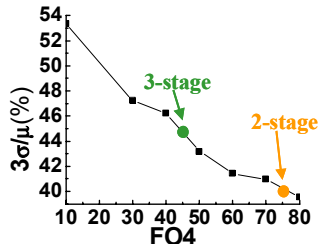


Figure 1. Delay variation with FO4 logic depth (SPICE)

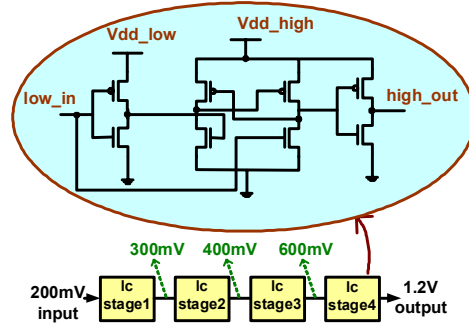


Figure 2. Level converter design

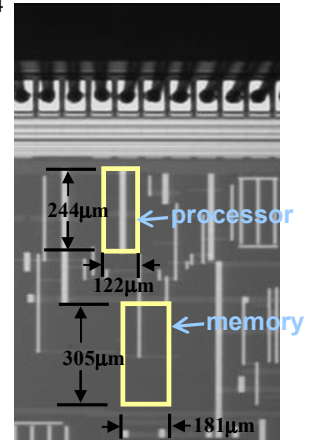


Figure 3. Die Photograph

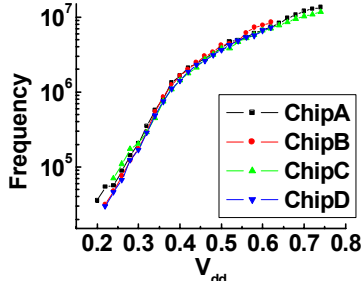


Figure 4. Measured frequency with V_{dd} for 4 processors

Table 1. Measured frequency distribution of 26 chips at different supply voltages

V_{dd}	μ (Freq)	$3\sigma / \mu$ (Freq)
0.260	84.66kHz	85.5%
0.400	1.529MHz	49.8%
0.600	6.759MHz	29.6%

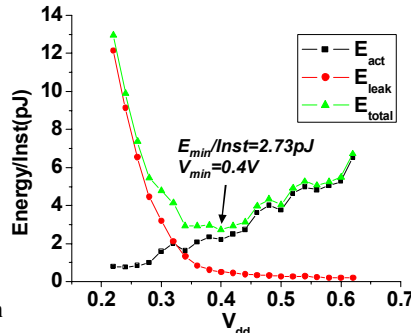


Figure 5. Dynamic, static and total energy for processor with V_{dd}

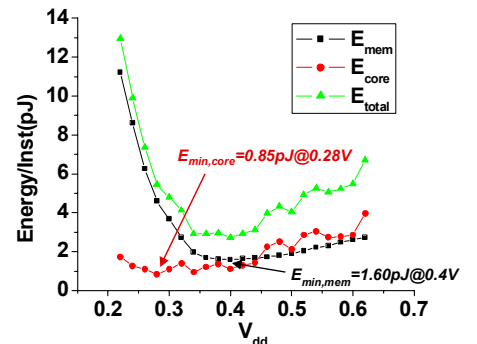


Figure 6. Energy with V_{dd} for the core and the memory

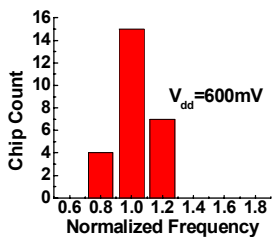
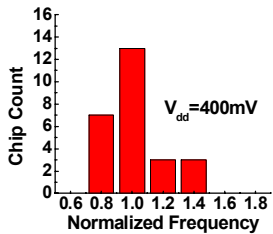
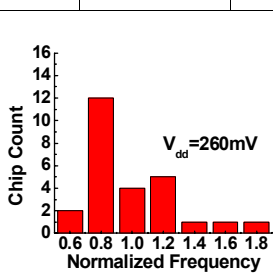


Figure 7. Process variation with voltage

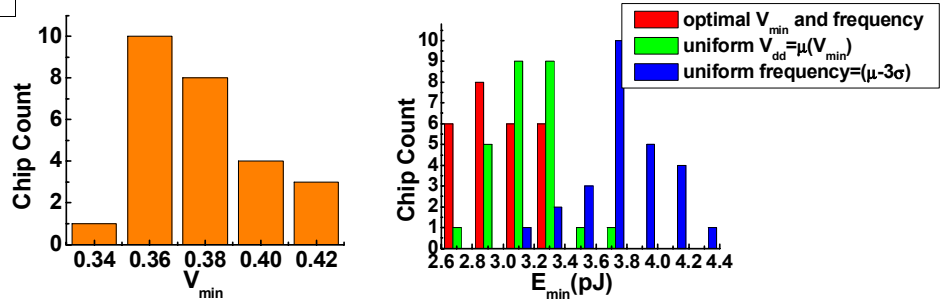


Figure 8. V_{min} and E_{min} distribution

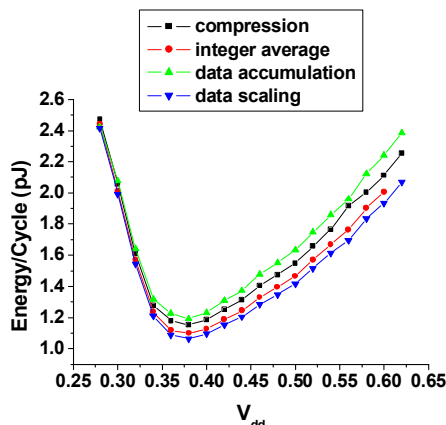


Figure 9. Energy efficiency with V_{dd} for 4 sensor applications

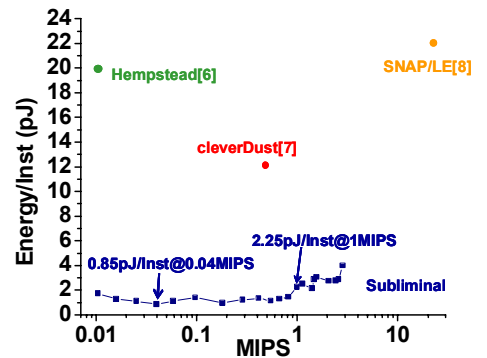


Figure 10. Energy efficiency trade-off against MIPS for subliminal core and comparison to previous work